

Hydration in Weak Polyelectrolyte Brushes

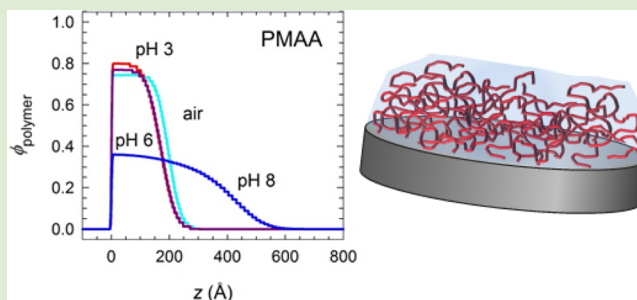
Chaitra Deodhar,[†] Erick Soto-Cantu,[†] David Uhrig,[‡] Peter Bonnesen,[‡] Bradley S. Lokitz,[‡] John F. Ankner,^{*,§} and S. Michael Kilbey, II^{*,†,‡}

[†]Department of Chemistry, University of Tennessee, Knoxville, Tennessee 37996, United States

[‡]Center for Nanophase Materials Sciences and [§]Spallation Neutron Source, Oak Ridge National Laboratory, Oak Ridge, Tennessee 37831, United States

Supporting Information

ABSTRACT: Weak polyelectrolytes (PEs) are complex because intertwined connections between conformation and charge are regulated by the local dielectric environment. While end-tethered PE chains—so-called PE “brushes”—are archetypal systems for comprehending structure–property relationships, it is revealed that the reference state nominally referred to as “dry” is, in fact, a situation in which the chains are hydrated by water vapor in the ambient. Using charge-negative PE homopolymer brushes based on methacrylic acid and copolymer brushes that incorporate methacrylic acid and 2-hydroxyethylmethacrylate, we determine self-consistently the water content of PE films using neutron reflectometry under different hydration conditions. Modeling multiple data sets, we obtain dry polymer mass density and layer thickness, independent of adsorbed water, and PE brush profiles into different pH solutions. We show that hydration of the chains distorts, here by as much as 30%, the quantification of these important physical parameters benchmarked to films in ambient conditions.



Wet and dry are concepts familiar to everyone. The ubiquity of liquid water on blue Earth and its remarkable properties as a solvent make hydration crucial to such disparate processes as lubrication,¹ adhesion and growth of biofilms,² partitioning and the fate of ions in soils,³ and protein folding and function.⁴ Assessing the degree of hydration is thus crucial to understanding how the nanoscopic structure of materials determines their macroscopic properties, yet, at the nanoscale, our comprehension of the role of water is far from complete.⁵ Most synthetic polymers encountered in everyday life, such as polystyrene, polyethylene, and polypropylene, are hydrophobic and thus by construction repel water and serve as barriers between different aqueous environments. Hydrophilic polymers, on the other hand, exhibit a much richer spectrum of interactions with the aqueous world.

Tethered polymer layers where the chains carry a significant number of ionizable groups and are covalently bound at one end to a surface are called polyelectrolyte (PE) brushes.^{6–21} Conceptually, they are important model systems because surface-sensitive probes can be brought to bear to study structure and properties that are inherently coupled because of interactions involving charges and polarization effects. Because of their responsive behavior, PE brushes play an important role in many areas of science and technology, such as colloid stabilization,⁶ adhesion, and lubrication.²² They can be used for designing biomaterial systems that improve the effectiveness of drug delivery or mediate cell/surface interactions to allow the control of the interaction of biological cells and biomolecules with artificial materials.²³ In such cases the polymer layer

properties are tuned to enhance the biocompatibility of an implant or to avoid nonspecific adsorption of proteins onto the active surfaces of an analytical device. Especially significant is the role of the areal (grafting) density of chains, which regulates interchain interactions and affects the local dielectric environment,^{7–12} thereby impacting the range and extent of interactions across the solid/fluid interface. Weak PEs are particularly complex in their behaviors because their degree-of-ionization is pH dependent and because added salt plays a dual role, affecting both the ionization state and screening charge.^{8,10,19–21}

We describe here a method for determining self-consistently, using neutron reflectivity, the degree of hydration of polyelectrolyte brushes and unambiguously determine basic physical properties of the brush layer as well as structural changes as a function of pH, a fundamental example of stimulus-responsive behavior. Hydrophilic polymer films equilibrated in air take up water from humid air and may indeed require it for structural stability. In such situations, the films are not dry, but rather, they are likely to be solvated. This has important consequences because not only does solvent water mediate interactions involving charges but also the presence of this adsorbed water complicates any characterization that aims to quantify layer thickness d , grafting density

Received: November 20, 2012

Accepted: April 19, 2013

Published: April 24, 2013

of polymer chains Γ , or the mass density of the polymer layer ρ because these parameters are intimately linked through the dimensional expression

$$\Gamma = \rho d N_A / M_n \quad (1)$$

where M_n is the number-average polymer molecular weight and N_A is Avogadro's number. This interplay is even more complex in weak PEs because, as alluded to earlier, they have the ability to regulate their structure locally, thereby changing their properties, through trade-offs in chemical (acid–base) equilibrium and physical interactions such as charge screening based on the local dielectric environment.^{7–9,11,19–21,24} Common approaches for determining Γ involve measuring film thickness using optical ellipsometry, assuming values for film density and refractive index,^{10,18,23} or using atomic force microscopy.¹⁷ While neutron reflectometry has been used to examine the nanoscale structure of strong as well as weak PE brushes,^{14–16} none of the previous neutron reflectometry studies have accounted rigorously for the presence of adsorbed water in polyelectrolyte films. We posit that this accounting is critical for understanding structure–property relationships because without knowledge of the amount of adsorbed water any calculation of layer thickness, grafting density, or film density is in error. Thus, only by taking into account the latent hydration in polymer films can one know the amount of polymer in these films.

In this Letter, we determine the pH-dependent structure of weak polyelectrolyte brushes, taking into account in a self-consistent manner the amount of adsorbed water. We introduce the concept of a “dry” thickness of polymer of a given density, which represents the material that is truly conserved upon exposure to different buffer solutions and humid air. This polymer inventory is established using neutron reflectometry measurements in humid air and in a liquid/solid solution cell in contact with deuterated water (D_2O) buffer solutions at pH 3, 6, and 8 (constituted to be 10 mM using NaCl as the added salt to control ionic strength, as described in the Supporting Information). Weak polyelectrolyte brushes made of poly(methacrylic acid) and also random copolymer brushes consisting of methacrylic acid (MAA) and hydroxyethyl methacrylate (HEMA) were studied. As described in the Supporting Information, these polymer brushes were synthesized using surface-initiated atom transfer radical polymerization (SI-ATRP). Brushes were grown from silicon substrates (50 mm diameter, 5 mm thickness) that were first functionalized with the initiator, 2-bromo-*N*-(11-(dichloro(methyl)silyl)undecyl)-2-methylpropanamide. To alleviate problems with polymerization of the reactive electrolytic form of MAA,¹⁰ brushes were made by chemical conversion of neutral, precursor brushes comprised of *tert*-butyl methacrylate (tBMA). Random P(MAA_{1–*r*}-*co*-HEMA_{*r*}) brushes identified by the mole fraction *r* of HEMA were also synthesized. Chains simultaneously grown from sacrificial initiator in free solution were recovered and characterized by size exclusion chromatography. (See Supporting Information for details.)

To understand the role of water in PE brushes, we must explicitly account for its presence and its effect on the measured neutron reflectivity. The mass *m* of a film is given by $\rho A d$, the product of mass density ρ , area *A*, and thickness *d*. Area *A* is not intrinsic to the polymer, but mass per area μ is:

$$\mu = m/A = \rho d \quad (2)$$

Neutron scattering-length density (SLD) likewise depends on ρ :²⁵

$$\Sigma = \sum_{j=1}^J b_j/V = \rho N_A \sum_{j=1}^J b_j/M \equiv \rho S \quad (3)$$

where *M* is the molar mass of the *J* atoms in the compound (e.g., monomer) composed of nuclei of scattering length *b_j*. Since stoichiometry *S* is known, but mass density ρ may not be, we separate them. The SLD of a layer composed of tethered polymer containing adsorbed water may be written as a volume-fraction weighted sum of the constituent SLDs:

$$\Sigma_{\text{hum}} = f_{\text{hum}} \Sigma_{\text{H}} + (1 - f_{\text{hum}}) \rho S \quad (4)$$

where f_{hum} is the volume fraction of water in the film, Σ_{H} the SLD of water, and ρS the SLD of the polymer. If the adsorbed water does not react with the polymer and maintains its bulk density, then it may be assumed to swell the film

$$\mu/\rho = (1 - f_{\text{hum}}) d_{\text{hum}} \quad (5)$$

where d_{hum} is the fitted thickness of the swollen hydrated film and μ/ρ can be understood as the dry thickness of polymer in the absence of adsorbed water [recall eq 2]. A neutron reflectivity measurement of the film in humid air will yield two fitted parameters d_{hum} and Σ_{hum} , but eqs 4 and 5 contain *three* unknown quantities: ρ , μ/ρ , and f_{hum} . One must therefore perform at least one additional measurement under different hydration conditions, for example, against a pH-controlled D_2O buffer solution:

$$\Sigma_{\text{pH}} = f_{\text{pH}} \Sigma_{\text{D}} + (1 - f_{\text{pH}}) \rho S \quad (6)$$

$$\mu/\rho = (1 - f_{\text{pH}}) d'_{\text{pH}} \quad (7)$$

yielding four equations (Σ_{D} being the SLD of D_2O) to solve for the four unknown quantities ρ , μ/ρ , f_{hum} , and the volume fraction of D_2O in the film against the buffer solution, f_{pH} . The reduced thickness d'_{pH} accounts for the fact that polymer brushes often exhibit volume-fraction profiles φ that are observably not “slab-like”, but smoothly decaying, such as the modified parabola, a phenomenological shape derived from a theoretical treatment of uncharged brushes,²⁶

$$\varphi(z) = (1 - f_{\text{pH}}) [1 - (z/d_{\text{pH}})^2]^\alpha \quad (8)$$

where varying $0 \leq \alpha \leq 1$ changes the shape of the profile continuously from block ($\alpha = 0$) to parabola ($\alpha = 1$). For such a profile

$$d'_{\text{pH}} \approx (1 - \alpha/3) d_{\text{pH}} \quad (9)$$

because mass balance requires that the area under $\varphi(z)$ be preserved.²⁷ The equations above may be solved for the four parameters of interest and written in forms more impressive for length than clarity, as shown in the Supporting Information. The most compact is the expression for the mass density of the dehydrated polymer film:

$$\rho = \frac{1}{S} \frac{\Sigma_{\text{D}}(\Sigma_{\text{H}} - \Sigma_{\text{hum}})d_{\text{hum}} - \Sigma_{\text{H}}(\Sigma_{\text{D}} - \Sigma_{\text{pH}})d'_{\text{pH}}}{(\Sigma_{\text{H}} - \Sigma_{\text{hum}})d_{\text{hum}} - (\Sigma_{\text{D}} - \Sigma_{\text{pH}})d'_{\text{pH}}} \quad (10)$$

Neutron reflectivity measurements were made at the Spallation Neutron Source (SNS) at Oak Ridge National Laboratory using the Liquids Reflectometer (LR). By collecting specular reflectivity data using a continuous wavelength band

($2.5 \text{ \AA} < \lambda < 6.0 \text{ \AA}$) at several different incident angles (here $\theta = 0.19^\circ, 0.27^\circ, 0.34^\circ, 0.48^\circ, 0.62^\circ, 1.11^\circ$, and 2.01°), data were acquired over a wavevector transfer ($Q = 4\pi \sin \theta/\lambda$) range of $0.006 \text{ \AA}^{-1} < Q < 0.176 \text{ \AA}^{-1}$. Setting the incident beam slits at each angle to maintain a constant relative wavevector resolution of $\delta Q/Q = 0.02$ allows the data obtained at different θ to be stitched together into a single reflectivity curve. The neutron refractive index depends on the SLD. To model the measured reflectivity, layer compositions, thicknesses, and interfacial widths were adjusted to optimize goodness-of-fit.²⁸ Samples were measured in air and against 10 mM buffer solutions at pH 3, 6, and 8 made using D_2O .²⁹ Reflectivity measurements in buffer solutions were performed using an inverted geometry, with neutrons incident on the brush/solution interface through the silicon substrate. Figure 1 shows neutron reflectivity data

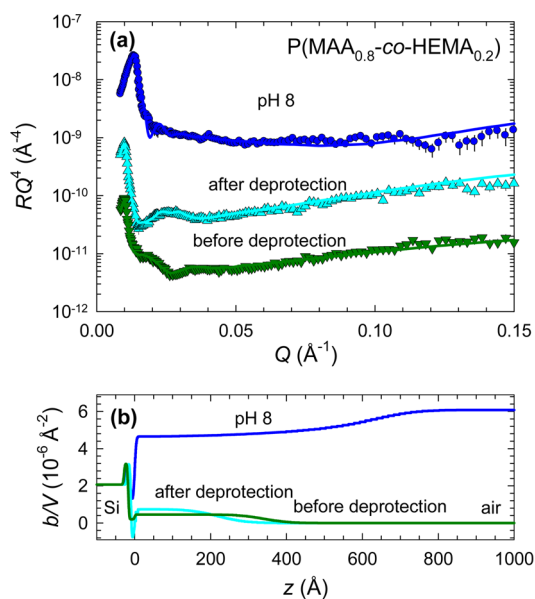


Figure 1. Reflectivity curves RQ^4 vs wavevector Q (a) and fitted scattering density profiles (b) for an $r = 0.2$ random copolymer film before deprotection [$\text{P}(t\text{BMA}_{0.8}\text{-co-HEMA}_{0.2})$] and after deprotection [$\text{P}(\text{MAA}_{0.8}\text{-co-HEMA}_{0.2})$] in humid air and against a pH 8 buffer solution (10 mM) made with D_2O . Curves shown in (a) are shifted vertically for clarity.

and model fits for a random copolymer film ($r = 0.2$) composed of 80% MAA and 20% HEMA monomers [$\text{P}(\text{MAA}_{0.8}\text{-co-HEMA}_{0.2})$]. Upon deprotection, the film thickness decreases, and the SLD increases, indicative of the replacement of *tert*-butyl groups (C_4H_9) by protons. For pH values above the MAA isoelectric point, the film expands into the solution (pH 8). As can be seen from the profiles in Figure 1(b), changes to the SLD profile may be subtle and will vary depending on the subphase. In addition, one must account in the model for the native silicon oxide and polymer initiator layers.

For clarity, in Figure 2, we depict polymer volume fraction profiles derived from fits like those shown in Figure 1, rather than the less intuitive, more cluttered SLD profiles. Shown are profiles for $r = 0, 0.2$, and 0.3 random copolymer films measured in the ambient and against pH 3, 6, and 8 D_2O buffer solutions. The inset to Figure 2(c) depicts the MAA and HEMA monomers and their random association in the polymer. At first glance, the variation in thicknesses of the polymer layers measured in humid air stands out. With an areal

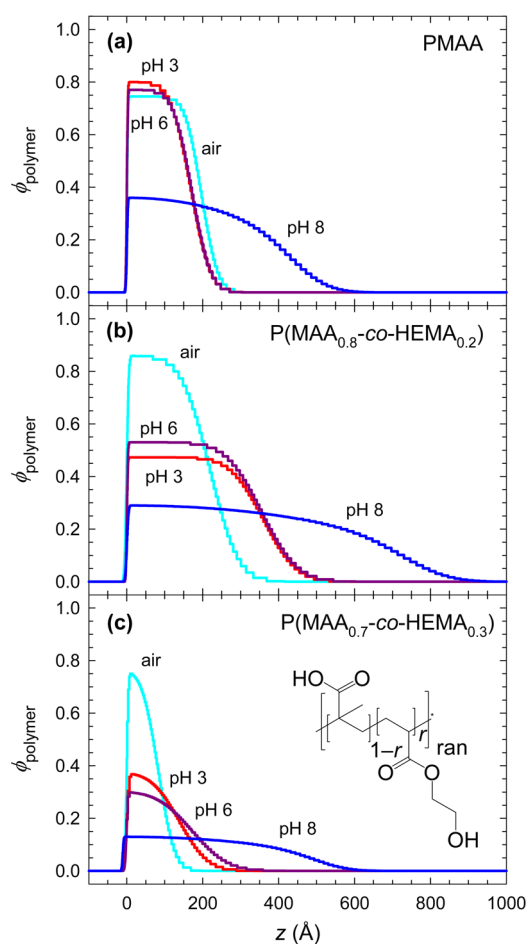


Figure 2. Fitted random copolymer $\text{P}(\text{MAA}_{1-r}\text{-co-HEMA}_r)$ volume fraction profiles for (a) $r = 0$, (b) $r = 0.2$, and (c) $r = 0.3$ for films measured in air and the same films in contact with pH 3, 6, and 8 D_2O buffer solutions at 10 mM ionic strength. The inset in (c) schematically represents MAA and HEMA monomers and their random association in the polymer.

density of initiators on the order of 10^{17} cm^{-2} , a low number of radicals are generated in SI-ATRP, making growth of these brushes highly sensitive to surface preparation and polymerization conditions and difficult to control,¹⁰ so a certain amount of thickness variation is unavoidable. Surface roughnesses in excess of $\sigma_{\text{fwhm}} = 80 \text{ \AA}$ were measured for all of the films,³⁰ a consequence both of surface-preparation sensitivity and of the natural stochastic thickness variation of films grown from surface initiator layers on large-diameter (50 mm) wafers. Nonetheless, the swelling response of the PE brushes exhibits clear trends with increasing HEMA fraction r and pH. Upon exposure to buffer solution, the pure PMAA film remains collapsed until pH 8, while both of the HEMA-containing copolymers initially swell at pH 3 and pH 6 before further expanding at pH 8. Degree-of-swelling increases both with increasing r and with pH. The apparent shift in the pK_a of the PMAA, manifest in the collapsed-to-swollen transition that occurs between $6 < \text{pH} < 8$, is striking; however, it is consistent with the shift to higher pH values Ober et al. determined using contact angle titration experiments, which probe the periphery of the film.¹³ This shift arises because, as stated previously, the PMAA chains locally regulate their degree-of-dissociation based on the local dielectric environment.

Table 1. Results of Iterative Fitting of the Neutron Data^a

<i>r</i>	pH	<i>f</i> _{pH}	<i>f</i> _{hum}	ρ (g/cm ³)	μ/ρ (Å)	stretch ratio	Γ_{neutron} (10 ⁻² Å ⁻²)
0	3	0.16	0.27 ± 0.01	1.04 ± 0.03	142.5 ± 2.7	1.3	0.17 ± 0.01
	6	0.19				1.3	
	8	0.62				2.8	
0.2	3	0.50	0.15 ± 0.03	0.91 ± 0.06	187.5 ± 6.7	2.0	0.22 ± 0.01
	6	0.46				2.0	
	8	0.72				3.5	
0.3	3	0.60	0.31 ± 0.03	1.01 ± 0.06	57.4 ± 2.3	2.6	0.13 ± 0.01
	6	0.68				3.2	
	8	0.87				7.8	

^aHere, *r* is the mole fraction of HEMA in the random copolymer, *f*_{pH} the water volume fraction in the copolymer against D₂O pH buffer, *f*_{hum} the volume fraction of water in the polymer film in humid air, ρ the mass density of the polymer, μ/ρ the polymer “dry” thickness in the absence of hydrating water. The stretch ratio is wet vs dry thickness, $d'_{\text{pH}}/(\mu/\rho)$, and Γ_{neutron} is the neutron-derived grafting density.

The qualitative observations of the pH-induced swelling behaviors are borne out by the models. Fitted parameters are listed in Table 1. In fitting the neutron reflectivity data for different backing media, we employed an ad hoc self-consistent approach in which we held dry polymer mass density ρ and thickness μ/ρ constant across the solvent series, determining water content and profile shapes in an iterative process. In future studies, self-consistency can be built explicitly into a model that fits all of the data sets simultaneously. Parameter uncertainties were determined statistically from the fitted individual solvent data sets. The uncertainty on the water volume fraction measured in air applies to all volume fraction values for a given sample. The water content of the films in humid air, *f*_{hum}, varies from 0.15 to 0.31, and while one might expect such variation between the three films prepared and measured over several months unless humidity is explicitly controlled, there appears to be an inverse correlation between *f*_{hum} and grafting density of chains, suggesting that less dense layers are able to take in more water. The sensitivity of brush thickness to changes in humidity was demonstrated by Biesalski and R  he,³¹ who used optical waveguide spectroscopy to show that the thickness of a cationic brush based on quaternized poly(4-vinylpyridine) increases dramatically (up to 40% increase) as the relative humidity of contacting air is increased. For all three films examined here, mass density ρ is close to 1 g/cm³, but dry thickness μ/ρ exhibits the growth-condition sensitivity discussed above. The stretch ratio between water-swollen and dry thicknesses, $d'_{\text{pH}}/(\mu/\rho)$ removes this variation, revealing a clear trend for greater swelling with increasing *r*. For all films, the shape parameter α was 0, indicative of collapsed block-like profiles, except at pH 8, where the data were best fit using $\alpha = 0.5 \pm 0.2$, producing the extended, tapered shape of the pH 8 profiles. The polymer grafting densities Γ_{neutron} were determined from eq 1 using fitted ρ and μ/ρ values.

The differences between structural parameters derived from constrained fits of neutron reflectivity data described above and those derived from ellipsometric measurement of film thickness in air (see Supporting Information) are significant. The greater film thickness and assumed mass density result in values of grafting density $\Gamma_{\text{ellipsometry}} = 0.22, 0.36, \text{ and } 0.23$ (10⁻² Å⁻²) for *r* = 0, 0.2, and 0.3, respectively. Clearly, using thicknesses of films hydrated by ambient moisture leads to overestimation of grafting densities and underestimation of stretch ratios, a conclusion also reached by Biesalski and R  he in their studies of swelling behavior of a very thick brush.³¹ Due to the variation of film hydration in humid air, this discrepancy cannot easily be corrected in thin film systems. Only by explicitly

accounting for adsorbed water by a method similar to that described here can one accurately determine how much polymer is deposited on a surface and how much it expands in contact with solvent.

In summary, it is clear that material characterization begins with proper accounting. This is particularly important in PE brush systems, where grafting density establishes the local dielectric environment^{7-9,11,19-21} and sets the balance between intra- and interchain interactions, which govern chain extension and thus the range of interactions across a brush-modified interface. Control of these characteristics is central to the utility of brushes as surface-modifying agents. Moreover, it is fully expected that water-soluble thin films in general suffer the same ambiguity between grafting density, mass density, and thickness if measured in the ambient using conventional benchtop methods such as ellipsometry, atomic force microscopy, or quartz crystal microbalance techniques only. While these methods are useful in their own right, the ability of neutron scattering to discriminate between adsorbed water and native polymer chains while simultaneously providing insight into nanoscale structural behaviors offers an important advantage for determining parameters that control structure and physical behaviors of PE brushes and other water-swellaible thin films.

■ ASSOCIATED CONTENT

📄 Supporting Information

Details of the initiator and polymer syntheses and characterizations, recipes for buffer solutions, and a complete derivation of hydration parameters. This material is available free of charge via the Internet at <http://pubs.acs.org>.

■ AUTHOR INFORMATION

Corresponding Author

*E-mail: mkilbey@utk.edu or anknerj@ornl.gov.

Notes

The authors declare no competing financial interest.

■ ACKNOWLEDGMENTS

Materials synthesized at CNMS, which is sponsored at Oak Ridge National Laboratory by the Office of Basic Energy Sciences, U.S. Department of Energy, were provided through User Project 2011-055. SMKII, CD, and ESC gratefully acknowledge support from the National Science Foundation through the Chemical, Bioengineering, Environmental and Transport program (Grant nos. 0840249 and 1133320). Neutron reflectometry measurements were performed at the

SNS at ORNL, managed by UT-Battelle, LLC for the DOE under Contract No. DE-AC05-00OR22725.

■ REFERENCES

- (1) Chen, M.; Briscoe, W. H.; Armes, S. P.; Klein, J. *Science* **2009**, *323*, 1698.
- (2) Bos, R.; van der Merwe, H. C.; Busscher, H. S. *FEMS Microbiol. Rev.* **1999**, *23*, 179.
- (3) Lee, S. Z.; Allen, H. E.; Huang, C. P.; Sparks, D. L.; Sanders, P. F.; Peijnenburg, W. J. G. M. *Environ. Sci. Technol.* **1996**, *30*, 3418.
- (4) Kovacs, I. A.; Szalay, M. S.; Csermely, P. *FEBS Lett.* **2005**, *579*, 2254.
- (5) Water – From Interfaces to the Bulk. *Faraday Discussions 141*; Heriot-Watt University, Edinburgh, U.K., August 27–29, 2008.
- (6) Pincus, P. *Macromolecules* **1991**, *24*, 2912.
- (7) Kumar, R.; Sumpter, B. G.; Kilbey, S. M. *J. Chem. Phys.* **2012**, *136*, 234901.
- (8) Gong, P.; Genzer, J.; Szleifer, I. *Phys. Rev. Lett.* **2007**, *98*, 018302.
- (9) Gong, P.; Wu, T.; Genzer, J.; Szleifer, I. *Macromolecules* **2007**, *40*, 8765.
- (10) Sankhe, A. Y.; Husson, S. M.; Kilbey, S. M. *J. Polym. Sci., Part A: Polym. Chem.* **2007**, *45*, 566.
- (11) Tagliazucchi, M.; de la Cruz, M. O.; Szleifer, I. *Proc. Natl. Acad. Sci.* **2010**, *107*, 5300.
- (12) Witte, K. M.; Kim, S.; Won, Y. Y. *J. Phys. Chem. B* **2009**, *113*, 11076.
- (13) Dong, R.; Lindau, M.; Ober, C. K. *Langmuir* **2009**, *25*, 4774.
- (14) Muller, F.; Romet-Lemonne, G.; Delsanti, M.; Mays, J. W.; Daillant, J.; Guenoun, P. *J. Phys.: Condens. Matter* **2005**, *17*, S3355.
- (15) Mir, Y.; Auroy, P.; Auvray, L. *Phys. Rev. Lett.* **1995**, *75*, 2863.
- (16) Tran, Y.; Auroy, P.; Lee, L.-T. *Macromolecules* **1999**, *32*, 8952.
- (17) Tugulu, S.; Barbey, R.; Harms, M.; Fricke, M.; Volkmer, D.; Rossi, A.; Klok, H.-A. *Macromolecules* **2007**, *40*, 168.
- (18) Konradi, R.; Rühle, J. *Macromolecules* **2005**, *38*, 4345.
- (19) Israëls, R.; Leermakers, F.A. M.; Fleer, G. J. *Macromolecules* **1994**, *27*, 3087.
- (20) Lyatskaya, Yu. V.; Leermakers, F.A. M.; Fleer, G. J.; Zhulina, E. B.; Birshtein, T. M. *Macromolecules* **1995**, *28*, 3562.
- (21) Zhulina, E. B.; Birshtein, T. M.; Borisov, O. V. *Macromolecules* **1995**, *28*, 1491.
- (22) Klein, J.; Kamiyama, Y.; Yoshizawa, H.; Israelachvili, J. N.; Fredrickson, G. H.; Pincus, P.; Fetters, L. J. *Macromolecules* **1993**, *26*, 5552.
- (23) de Vos, W. M.; Biesheuvel, P. M.; de Keizer, A.; Kleijn, J. M.; Cohen Stuart, M. A. *Langmuir* **2008**, *24*, 6575.
- (24) Manning, G. S. *J. Chem. Phys.* **1969**, *51*, 924.
- (25) Penfold, J.; Thomas, R. K. *J. Phys.: Condens. Matter* **1990**, *2*, 1369.
- (26) Karim, A. .; Satija, S. K.; Douglas, J. F.; Ankner, J. F.; Fetters, L. J. *Phys. Rev. Lett.* **1994**, *73*, 3407.
- (27) The integral of $\varphi(z)$ is a hypergeometric function. See: Gradshteyn, I. S.; Ryzhik, I. M. *Table of Integrals, Series, and Products*, seventh ed.; Academic Press: New York, 2007.
- (28) Russell, T. P. *Phys. B* **1996**, *221*, 267.
- (29) Rahane, S. B.; Floyd, J. A.; Metters, A. T.; Kilbey, S. M., II *Adv. Funct. Mater.* **2008**, *18*, 1232.
- (30) The full-width-at-half-maximum roughness is ~ 2.35 times larger than the more commonly used Gaussian standard deviation.
- (31) Biesalski, M.; Rühle, J. *Langmuir* **2000**, *16*, 1943.